Metallurgy and materials

Characterization of micro resistance spot welding on aluminum electrolytic capacitors

http://dx.doi.org/10.1590/0370-44672023780156

Weslen Rosiak Lopes[1,3]
https://orcid.org/0009-0005-7568-2215
Hugo Marcelo Veit[2,4]
https://orcid.org/0000-0002-8843-8466

[1]Universidade Federal do Rio Grande do Sul – UFRGS, Programa de Pós-Graduação em Engenharia de Minas, Metalúrgica e de Materiais (PPGE3M), Porto Alegre - Rio Grande do Sul – Brasil.

[3]Universidade Federal do Rio Grande do Sul – UFRGS, Departamento de Engenharia de Materiais, Porto Alegre - Rio Grande do Sul – Brasil.

E-mails: [3]weslen.lopes@icloud.com, wes.rlopes@gmail.com, [4]hugo.veit@ufrgs.br

Abstract

Resistance spot welding (RSW) processes are applied across a diverse range of manufacturing processes in industry with the objective of permanently joining two metal parts. RSW occurs due to heat generated on focal points by the resistance that an electric current flow (AC or DC) encounters when passing through metallics pieces pressed against each other by electrodes. This study is based on a design of experiments (DOE), focused on the manufacture of aluminum electrolytic capacitors, and seeks to characterize the influence of RSW parameters (electrical current density, weld time and electrodes pressure) on the tensile strength of the weld joint formed between aluminum alloy AW3003 and a low carbon steel sheet coated with copper and tin by electrodeposition. The DOE consists of a sweep on the electrical current between 12kA and 20kA, weld times 8ms and 12ms and pressures 0.3Mpa and 0.4Mpa. The welding interface of the specimens was also analyzed by SEM and EDS, revealing different types of morphologies. The results obtained highlighted the electrical current as the main influence factor on the tensile strength, also enabling the identification of different types of morphology on welding interface. The observed tensile strength results for the studied parameters ranged from 376N to 1095N (average), and an optimized combination of parameters based on a statistical analysis in Minitab software is suggested at 18kA, 12ms and 0.3Mpa.

Keywords: resistance spot welding, aluminum, steel, copper, electronics.

1. Introduction

Due to their high welding efficiency and applicability to weld a diverse range of dissimilar metals, resistance spot welding (RSW) processes have become essential in the automotive industry, especially during the transition from heavy materials to light alloy materials, which reduces the car's weight and results in notable benefits, such as better fuel efficiency, improved performance, and lower environmental impacts by CO_2 reduction. (Park, Y-D; karim, M. A., 2020; Zhang, W. *et al.*, 2019). From the emergence of the technology, several adaptations and improvements began to be made to apply the concept to other areas, such as the fabrication and assembly of the lithium-ion cell batteries through application of micro resistance spot welding (MRSW) with the objective of performing the joining of thin parts (Gopalan, R. *et al.* , 2020). It is considered MRSW when the parts to be welded have less than 1mm of thickness. This welding method became very important due to the trend to miniaturization of complex microsystems, demanding high precision and high quality (Baskoro, A. S. *et al.*, 2016). MRSW is also widely used for the assembling of aluminum electrolytic capacitors of the type axial soldering star, providing vibration stability without additional requests of clamping on printed circuit boards (PCB) due to the rugged plates (negative terminals) welded on the capacitor case. As seen on Figure 1, the soldering star, besides being the negative terminals from the capacitor, works as a base to place the capacitor on PCB and realize the final weld that will fix the component on the circuit definitively. The application of these capacitors in the field requires a high reliability level of the welding joint, since they need to withstand high vibration loads added to a rapid change of temperature (eg: capacitors mounted next to the engine).

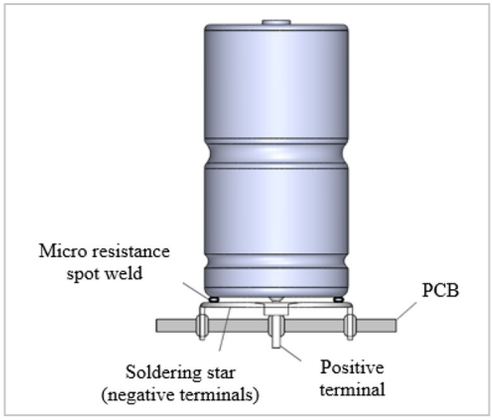

Figure 1 - Soldering Star Capacitor Welded on a PCB (printed circuit board).

In general, RSW and MRSW are joining processes that occur by a dense flow of electrical current (AC or DC) from a power source to the electrodes and across the metallic parts being pressed against each other by the electrodes themselves. When the welding current passes through the contact resistances between both parts, heat is generated by effect of the joule principle, increasing the temperature and producing the joining (Brandi, S. D., 1992). There are important parameters to be controlled to have a high-quality weld joint, mainly electrical current density, weld time, pressure of the electrodes and electrode design (Wu, S-N. *et al.*, 2014). Several studies in this field used to be performed seeking optimized combinations of parameters to improve the welding joint. The results from these studies show a direct correlation between electrical current and welding time to the area welded. The greater the current and time, the greater is the area welded, consecutively increasing the tensile strength of the joint (Mikno, Z.; Kowieski, S, 2019). The electrical and thermal contact resistance is primordial for heat generation on a focused area. This resistance varies according to contact pressure, temperature, surface roughness, oxide layers and organic contaminations (Osvald, J. *et al.*, 2023). For some cases, it is necessary to focus the heating on some strategic points. It is usual to have one or more welding projections, normally of spherical shape, to reduce the area of the current flow and increase the contact resistance. This necessity for welding projections used to occur due to the volume difference between the parts to be welded; it is advisable for differences greater than 5:1 (Amada Weld Tech Inc., 2020). An advantage to be considered by using welding projection is the lesser energy demanded to heat the parts (Isotron. Resistance welding. 2023).

Depending on welding parameters and the material's base, different welding interfaces tend to be formed. A solid-state bond is normally obtained when using metals with different properties in terms of microstructure and melting point, one in relation to the other. In terms of welding parameter configuration, this type of connection is normally observed when there is a high electrical current in a short period of time. Due to the different material properties and short welding time, there is not necessarily a significant fusion of the two metals for the bonding to occur. However, there is a well-defined bond between the interface of the two metals, where a small intermetallic compound can be observed. The solid-state bond usually presents typically high mechanical resistance against shear and tensile strength. Opposite to the solid-state bond, exists the fusion bond, whose materials have similar properties and are heated up to the melting point, followed of a subsequent cooling that forms a nugget containing a mix from the materials welded. In this case, an intermetallic compound is clearly observed, presenting a greater thickness than an intermetallic compound obtained in solid state bonding. Fusion bonding can also present high mechanical resistance. However, depending on the materials involved, the intermetallic compounds formed can present unwanted mechanical properties, such as a decrease in the tensile resistance (Amada Weld Tech Inc., 2020).

There are mechanical tests to evaluate the quality of a welding joint, being the most usual, the tensile strength test. This test involves applying a controlled axial load to the specimen containing the welded joint, and gradually increasing it until the specimen fractures. The test measures several key parameters, including ultimate tensile strength, yield strength, elongation, and reduction in area. This tensile testing method provides valuable information about the mechanical behavior of the welded joint, helping to assess its quality and compliance with industry standards. (American Welding Society, 1997).

The aim of this study is to characterize the weld interface between the case and star base (negative terminals) on aluminum electrolytic capacitors of type axial soldering star according to different welding parameters listed in a DOE (design of experiment). Furthermore, to carry out tests of the tensile strength up to the rupture of the welding joint and measure the thermal zone affected (mark left by the soldering star on the aluminum case after detachment). Finding an optimized welding version can contribute substantially to the quality level of these components and avoid failures on vibration, since the resistance against vibration is a requirement of global standards, such as AEC (Automotive Electronics Council) and automotive customers (Thukral, V. *et al.*, 2022). Considering the challenge to weld metals with different properties (e.g. melting point, electrical conductivity, and thermal dissipation) in MRSW, the novelty of this study involves, a better understanding of which process parameter (electric current density, welding time and electrode pressure) is most significant for the manufacturing quality of aluminum electrolytic capacitors.

2. Materials and method

To investigate the influence of electrical current density, welding time and electrode pressure, a DOE was defined and then samples of aluminum electrolytic capacitors of the axial soldering type from the size Ø20x27mm (Figure 2) were produced for each combination of parameters possible. Table 1 refers to the parameters selected for this study.

Figure 2 – Example of sample produced.

Table 1 - DOE of welding parameters.

Version	Current [kA]	Time [ms]	Pressure [Mpa]	Version	Current [kA]	Time [ms]	Pressure [Mpa]
1	12	8	0.3	11	16	12	0.3
2	12	8	0.4	12	16	12	0.4
3	12	12	0.3	13	18	8	0.3
4	12	12	0.4	14	18	8	0.4
5	14	8	0.3	15	18	12	0.3
6	14	8	0.4	16	18	12	0.4
7	14	12	0.3	17	20	8	0.3
8	14	12	0.4	18	20	8	0.4
9	16	8	0.3	19	20	12	0.3
10	16	8	0.4	20	20	12	0.4

The equipment used to weld is a medium frequency inverter from ISOTRON, model CSMF-2, adapted to a special welding head. The electrodes are made of copper and are coupled to a pneumatic system that pressures the capacitor against the soldering star.

The soldering star is constituted of a plate clad with dissimilar materials composing three layers: its base material in the core is low carbon steel (< 0,10%) with 0.60mm of thickness (according to the manufacturer's specification), followed by an intermediate layer of copper, and a finishing layer of tin, each one having 9µm of thickness. On the soldering star, there exist 8 welding projections distributed along its circumference. Its shapes are convex, forming an angle of 120°. The case from the capacitor where the soldering star was welded is made of aluminum alloy AW3003.

After concluding the samples' production, 10 capacitors from each welding version were submitted to tensile strength tests, detaching the soldering star from the capacitor case, and measuring the force through a dynamometer from Mecmesin, model AFG 1000N. The thermal zone effect was also measured on a microscope from ZEISS, model Axio Zoom V16.

The welding interface was characterized by SEM using a Zeiss, model EVO LS 10 apparatus with energy-dispersive x-ray spectroscopy (EDS) mode. For this analysis, the samples were embedded with resin 818 (base of epoxy) and cured at 65°C for 24h. After curing, the specimens were polished with sandpapers of grits 600 (Al_2O_3), 1200 (SiC), 2500 (SiC), 3000 (SiC), 4000 (SiC) and 5000 (SiC) consecutively for 2 minutes for each sandpaper. Water was used as the lubricant, as well as a speed of 300RPM. At every step, the samples were cleaned with water flow and cotton. The finishing steps were performed with diamond pastes of grits 3µm, 1µm and 0.25µm for 5 minutes each one, with a speed of 150 RPM. During the change to diamond pastes, the samples were cleaned with ethyl alcohol in ultrasound.

One last metallographic characterization consisted of revealing the steel grain structure from the star after welding, close to the welding interface. The polished samples were etched with Nital (2%) reagent and analyzed on an optical microscope from Zeiss, model Lab. A1 Axio with magnification of 1000x.

3. Results and discussion

3.1 SEM and EDS results

From the data obtained by the SEM and EDS analyses, the spectrogram of the elements made it possible to observe that the tin (external layer from the soldering star) does not participate in the welding interface with significative proportions, independent of the parameters tested. The tin could only be detected with significative proportion around the welding points (Figure 3). A plausible justification for that is the melting point of the tin being the lowest compared to the other materials on the welding, and the high energy involved in the process makes the tin flow to the free areas around the joint.

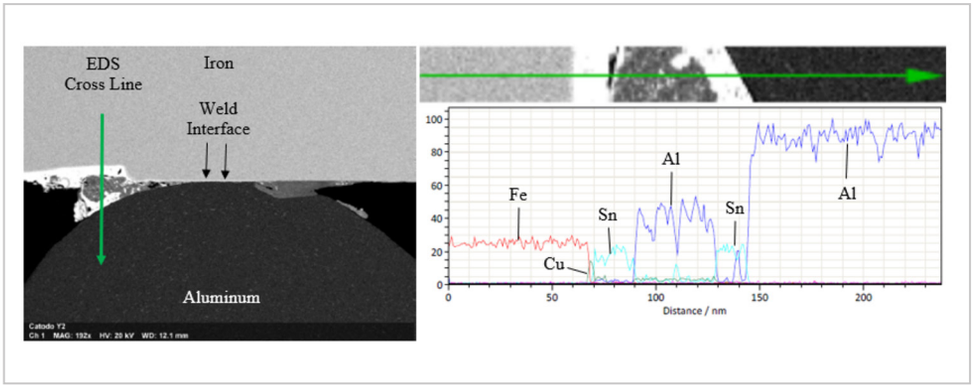

Figure 3 - EDS on segregated material (sample welded according to version 2).

The samples welded with 12kA and 14kA presented a welding interface majority between the aluminum and the copper (intermediate layer) from the soldering star. On this configuration, the tin was just found in insignificant proportions. This interface is similar to the solid-state bond, whereupon it is not possible to identify a large grain growth or IMC (intermetallic compound) greater than 1nm of thickness, suggesting that one or both materials did not reach the melting point, and the connection occurred through thermocompression. (Figure 4).

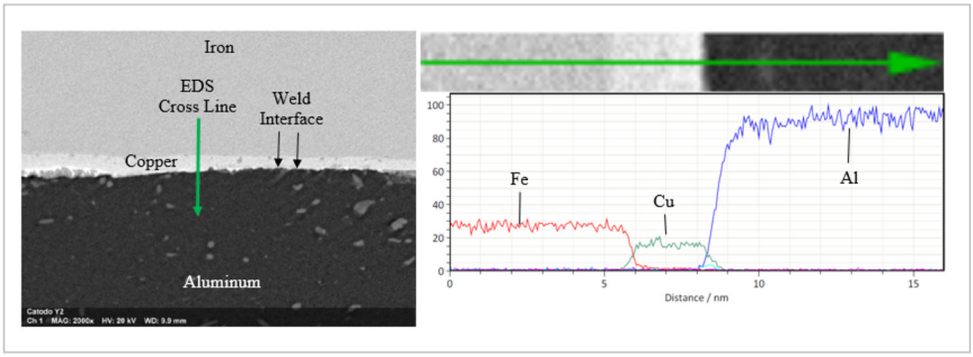

Figure 4 - EDS crossing the welding interface (sample welded according to version 8).

From 16kA, the same behavior observed on the tin starts to happen partially for the copper that was segregated around the thermal zone affected, opening contact between aluminum and steel (base material from the soldering star), resulting in a welding surface from both of these materials. This interface also presents characteristics from a solid-state bond formed by a thermocompression, with a layer growth thickness of 1nm as a result of the mixed aluminum and iron. If 18kA is applied, the copper is practically all segregated and the interface is in the most joined by solid state bond between aluminum and steel, as seen on Figure 5.

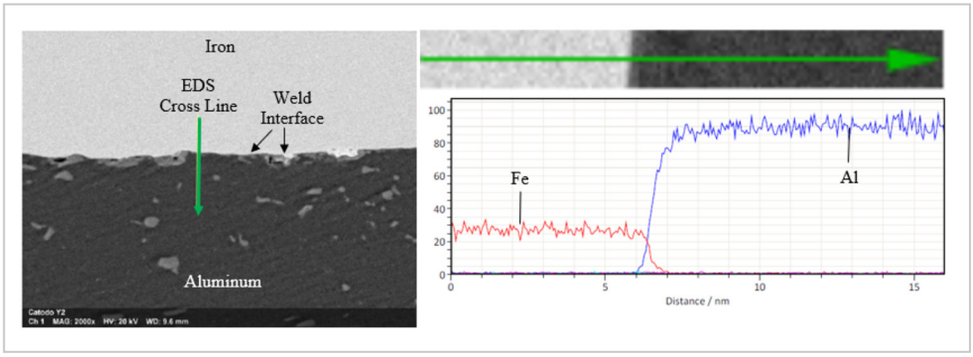

Figure 5 - EDS crossing the welding interface (sample welded according to version 16).

3.2 Tensile strength results

Figure 6 refers to the force necessary to rupture all welding points. In total, 10 parts from each welding version were submitted to the tensile strength test, and a trend towards the increase of mechanical resistance on the welding joints could be clearly seen, ranging from 284N to 1090N of average tensile resistance, according to the versions 1 and 20.

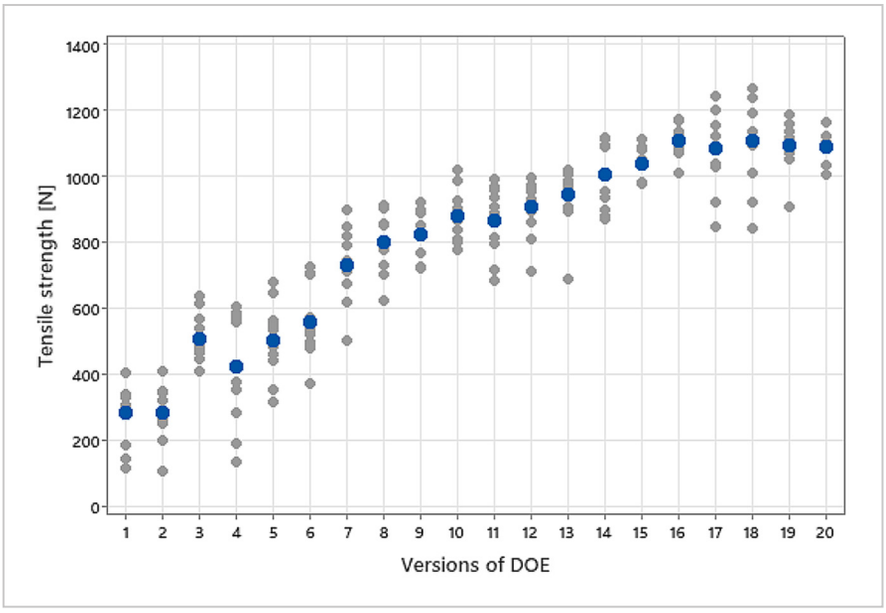

Figure 6 - Tensile strength test according to the versions from 1 to 20.

Figure 7 demonstrates the individually analyzed parameters (electrical current, welding time and electrode pressure) to investigate which of them is more significant to vary tensile strength. The lower the inclination of the lines, the lower the significance of the parameter. According to the levels of the parameters tested, the electrical current density showed to be substantially more representative compared to the welding time and electrode pressure. The average for the tensile strength changed from 376N to 1095N when the electrical current density was 12kA and 20kA, respectively. It is also important to note that the rate of tensile strength increase was almost constant between 12kA to 16kA, while from 16kA onward, the rate decreased. The reason for this is that the welded joint is exceeding the mechanical resistance of the materials welded, and even that should a higher current be applied, the tensile resistance may not increase more.

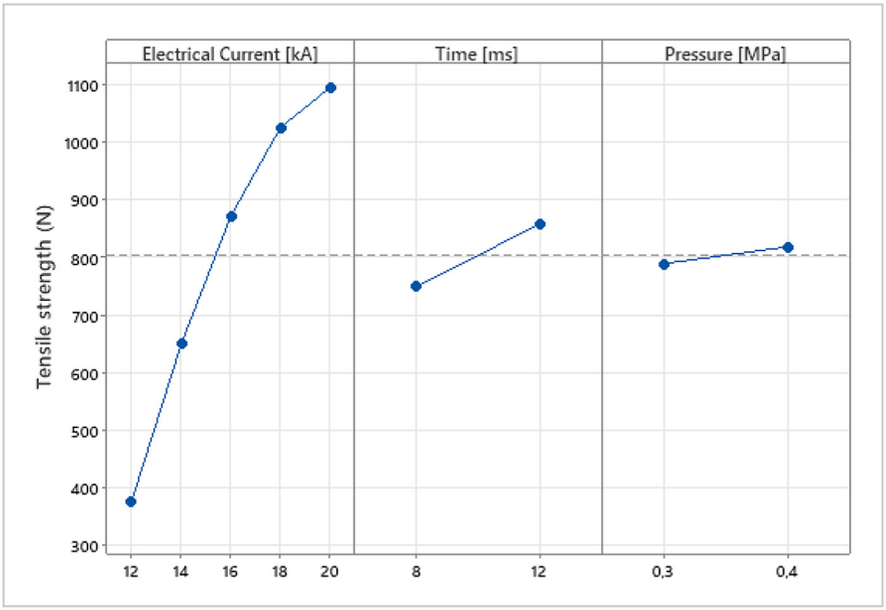

Figure 7 - Main effect analysis.

Another analysis was carried out to investigate the correlation between the tensile strength and welding area through the mark left by the soldering star onto aluminum case from the capacitor after detaching. The results obtained showed a direct correlation, whereby the greater the welded area, the greater the tensile strength of the welding joint (Figure 8). This analysis revealed higher ratio of thermal zone affected for the versions where the current was increased, while time and electrode pressure were not representative on this characteristic.

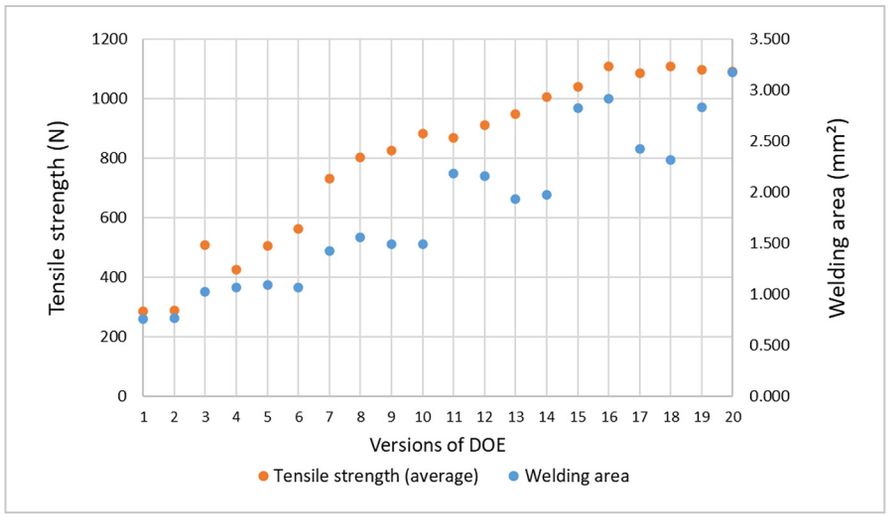

Figure 8 - Area printed on the aluminum after detaching soldering star.

The Figure 9 exemplifies two different cases observed during the tensile tests. From welding versions 1 to 13, the rupture by tensile occurs on the weld joint. From the version number 14 onward the center of some weld joints becomes stronger than mechanical resistance of aluminum, leading to the rupture of the capacitor case instead of the welding joint, although only some of the 8 welding projections present this behavior and tend to be randomized.

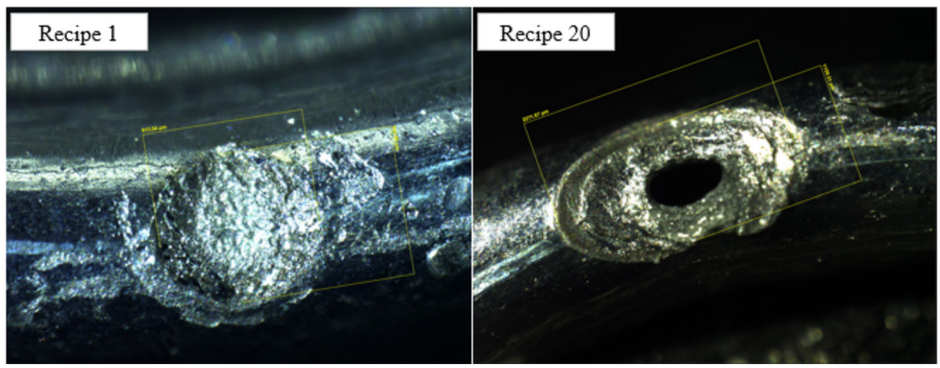

Figure 9 - Comparison between area printed by the version 1 and 20.

3.3 Grain structure results

Figure 10 defines the behavior of steel grain after welding with versions 8 (left) and 14 (right). From electrical current 16kA, it is possible to see a grain refinement through the size reduction of its contour (the grain size is smaller in version 14 than in version 8), which probably contributes to increase the mechanical resistance from the joint. Furthermore, the welded interface between aluminum and steel was proved again when a higher electrical current (≥ 16kA) was used to weld, segregating the copper to around thermal zone affected (in version 14 it is no longer possible to see the copper layer).

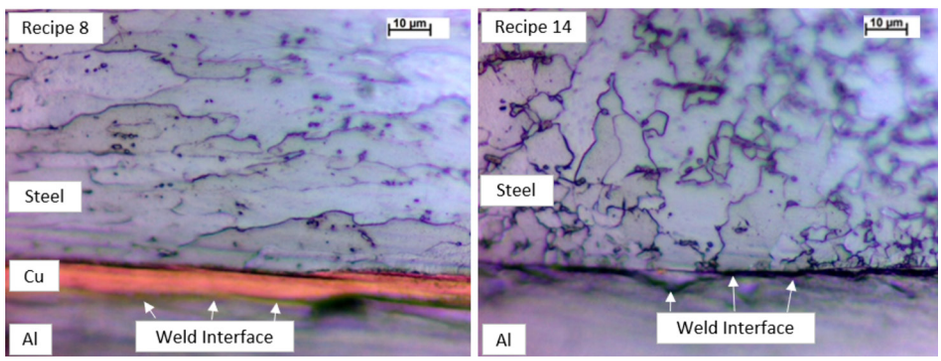

Figure 10 - Steel etched with Nital (2%) in versions 8 and 14.

4. Conclusions

Through this study, it was possible to find optimized welding versions to reach high levels of tensile strength and render the product more robust, besides identifying the relevance of each parameter. Three behaviors on the welded interface could be discovered according to the different levels of electrical current (main parameter). Between 12kA and 14kA, the weld

interface is substantially formed by copper and aluminum, presenting an average tensile strength resistance of respectively 376N and 649N. With 16KA, the copper starts to flow around the thermal zone, and there are welding interfaces formed by both steel and aluminum, and cooper and aluminum, presenting an average of tensile strength resistance of 872N. When the welding is performed with 18kA and 20kA, the interface is majority formed between steel with refined grain and aluminum, and its tensile strength resistance is respectively 1025N and 1095N. As a result of these last levels of welding energy, the joint is strong enough to not break, and what really breaks, is the aluminum from the capacitor case, indicating that the mechanical resistance of the welded joint exceeds the resistance of capacitor case. In addition to the different metals that are part of the welding interface, the area welded is also a factor that contributes to the increase in tensile strength. As the current density was increased, there was greater penetration of the welding's projection from the soldering star onto the capacitor, increasing the bonding area. Using all information of this study in a statistical analysis of DOE in Minitab software, the supposed welding parameter to be used seeking higher tensile strength with lower standard deviation must be the version 15 (18kA, 12ms and 0.3Mpa).

Independent of the welding version of this study, all welding interfaces were corresponded to a solid state bond and no intermetallic layer could be clearly detected. However, the EDS analysis had indicated, through the overlapping lines of materials found, the possibility of the existence of a thin layer of metals mixed on a thickness of approximately 1 nanometer, which could be associated to an intermetallic formation. The cause for this, can be the short welding time used in the study and the different properties of the materials, such as melting point, electrical conductivity, and thermal dissipation, which can contribute to the lack of reaching the melting point of the materials at the same time, and consequently, does not form a large growth of intermetallic compounds.

References

AMADA WELD TECH INC. Fundamentals of small parts resistance welding. 2020. Available at:<https://amadaweldtech.com/wp-content/uploads/2018/12/Resistance-Welding-Fundamentals.pdf> Access at: 16 dec. 2023.

AMERICAN WELDING SOCIETY. ***Welding Handbook***. 7 ed. USA: AWS, 1997. p. 371-373.

BASKORO, A. S. *et al*. The effect of welding time and welding currents on weld nugget and tensile properties of thin aluminum A1100 by micro resistance spot welding. Depok, Indonesia. ***Journal of Engineering and Applied Sciences,*** v. 11, p. 1050-1054, 2016.

BRANDI, S. D. ***Welding - processes and metallurgy.*** 11 ed. São Paulo: Editora Blucher, 1992. p. 217-240.

GOPALAN, R. *et al*. Tailoring micro resistance spot welding parameters for joining nickel tab to inner aluminum casing in a cylindrical lithium ion cell and its influence on electrochemical performance. Tamil Nadu, India. ***Journal of Manufacturing Processes,*** v. 49, p. 463-470, 2020.

ISOTRON. Resistance welding. 2023. Available at: <https://isotron.com.br/en/solda-por-resistencia/> Access at: 16 dec. 2023.

MIKNO, Z.; KOWIESKI, S. Micro-resistance spot welding of cylindrical battery packets in FEM calculations. Poland. ***Welding Technology Review,*** v. 91, p. 43-50, 2019.

OSVALD, J. *et al*. A computational and experimental study in resistance spot welding of thin-gauge and highly conductive dissimilar sheets for battery tab interconnects. Tempe, USA. ***Journal of Materials Processing Tech.,*** v. 322, p. 1-8, 2023.

PARK, Y-D; KARIM, M. A. A review on welding of dissimilar metals in car body manufacturing. Busan, Korea. ***Journal of Welding and Joining,*** v. 38, p. 8-19, 2020.

THUKRAL, V. *et al*. Board level vibration test method of components for automotive electronics: state-of-the-art approaches and challenges. Nijmegen, Netherlands. ***Journal Microelectronics Reliability,*** v. 139, p.1-11, 2022.

WU, S-N. *et al*. Microstructure characterization and quasi-static failure behavior of resistance spot welds of AA6111-T4 aluminum alloy. Chongqing, China. ***Transactions of Nonferrous Metals Society of China.,*** v. 24, p. 3879-3885, 2014.

ZHANG, W. *et al*. Dissimilar metal joining of aluminum to steel by ultrasonic plus resistance spot welding – microstructure and mechanical properties. Columbus, USA. ***Journal of Materials and Design,*** v. 165, p. 1-10, 2019.

Received: 8 January 2023 - Accepted: June 2024.